

# Effects of Electrodeposited Zinc Coating on the Formability of Drawing-Quality Aluminum-Killed Sheet Steel

J.L. Milián

Although sheet formability depends significantly on the properties of the base metal, surface coatings used for corrosion protection can affect the friction at the tool/sheet interface and, therefore, influence the amount of deformation. In an effort to better understand the effects of surface coatings on formability, limiting dome height testing was done on samples of drawing-quality aluminum-killed sheet steel with laboratory-produced electrodeposited zinc coatings of different characteristics. The results showed that the formability of zinc-coated products was reduced compared to the uncoated steel in all strain states. It was also shown that zinc coating crystallographic texture strongly influences sheet forming behavior and may be as important a parameter as surface roughness in friction characterization.

## 1 Introduction

PREVIOUS evaluation of commercially produced Zn, Fe-Zn, and Ni-Zn electrodeposited coatings on steel sheet revealed anomalies in forming behavior between the alloy-coated products that were attributed to differences in effective friction due to the different surface characteristics.<sup>[1]</sup> Although sheet formability depends significantly on the properties of the base metal, surface coatings can affect the friction at the interface and, therefore, influence the amount of deformation at the tool/sheet interface. In an effort to better understand the surface effects on formability, pure zinc coatings with four different surface characteristics were electrodeposited on samples from the same drawing-quality aluminum-killed (DQAK) sheet steel.

The limiting dome height (LDH) test<sup>[2]</sup> was then used to simulate the behavior of the zinc-coated sheet during forming. The limiting dome height test is a stretch-forming test that combines the effects of mechanical properties (the maximum amount of strain the metal can withstand before failure) and friction (how uniformly the strain is distributed) into a single numerical value. By keeping the substrate a constant, the effects due to the mechanical properties are held constant, and surface effects are isolated. Therefore, the limiting dome height values, or dome heights at failure, obtained from sheet with the four types of zinc coating can be compared among each other and with those obtained from the uncoated steel to detect frictional effects at the interface brought about by the different surfaces. A high limiting dome height value is then the result of low interface friction, which allows for uniform distribution of strain. Friction is known to be a function of hardness and rough-

ness of both tool and workpiece, lubrication regime, and forming mode.

## 2 Experimental Procedure

### 2.1 Material

Panels for this laboratory experiment were cut from a commercial coil of 0.74-mm (0.029-in.) thick cold rolled, aluminum-killed steel that had been continuously cast. Chemical

**Table 1** Composition of the Steel Substrate

Element	Composition, wt. %
C .....	0.040
Mn .....	0.29
P .....	0.013
S .....	0.009
Si .....	0.016
Cu .....	0.022
Ni .....	0.014
Cr .....	0.037
Mo .....	0.007
V .....	< 0.005
Ti .....	< 0.005
N .....	0.004
Nb .....	< 0.002
Al .....	0.053

**Table 2** Zinc Coating Characterization

Sample	Coating weight, g/m <sup>2</sup>	Coating thickness, μm	Knoop hardness(a)
Uncoated .....	0	0	154
A .....	60	15	55
B .....	60	15	39
C .....	100	25	67
D .....	100	26	50

(a) Knoop hardness number using 5-g load.

J.L. Milián, U.S. Steel Technical Center, Monroeville, Pennsylvania. The material in this article is intended for general information only. Any use of this material in relation to any specific application should be based on independent examination and verification of its unrestricted availability for such use and a determination of suitability for the application by professionally qualified personnel. No license under any USX Corporation patents or other proprietary interest is implied by the publication of this paper. Those making use of or relying upon the material assume all risks and liability arising from such use or reliance.

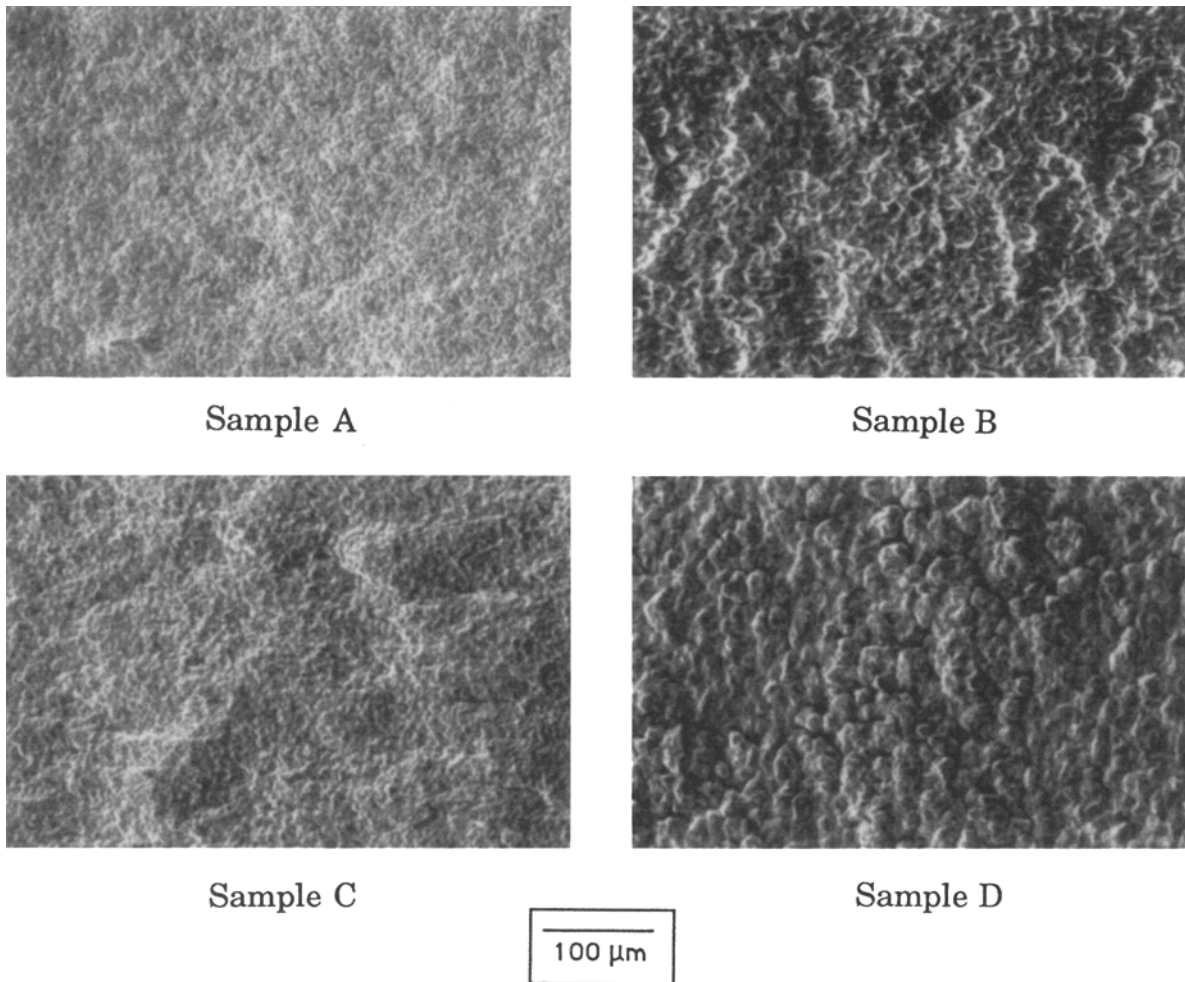


**Fig. 1** Scanning electron micrographs of the surface of as zinc-coated samples at 150 $\times$ .

analysis for this coil is given in Table 1. Pure zinc coatings were electrodeposited on one side of 8-by-12-in. panels using a chloride-base laboratory circulation cell, with the long axis in the rolling direction. Commercial plating conditions of a U.S. Steel proprietary electroplating process were simulated. Figures 1 and 2 show scanning electron microscope (SEM) photographs of the surface of the four different zinc coatings at two different magnifications. Table 2 lists the characteristics of the coatings. Microhardness measurements were taken on cross sections using a 5-g load. Surface roughness measurements were made using the Taylor-Hobson Surtronic 3 on the uncoated steel and the zinc-coated surfaces.

## 2.2 Mechanical Properties

The standard mechanical properties (yield strength, tensile strength, total elongation, and strain-hardening exponent, or  $n$  value) were determined by conducting tensile tests on longitudinal and transverse specimens obtained from three separate locations in a 0.74-mm (0.029-in.) thick temper rolled coil. The formability parameters ( $r_m$  and  $\Delta r$ ) were determined from tensile tests in the longitudinal, transverse, and 45 $^\circ$  directions. The

data reported are the result of duplicate tests at all conditions. Both coated and uncoated specimens were pulled.

## 2.3 X-Ray Measurements

Crystallographic texture was measured by X-ray diffraction techniques.<sup>[3]</sup> Integrated intensities were measured using filtered CuK $\alpha$  radiation and an automated scan of 2 $^\circ$  of 2 $\theta$  for each reflection. The relative intensities of X-ray reflections from a polygranular zinc sample without any texture, or random orientation, were taken from the ASTM/JCPDS card No. 4-0831. For three-dimensional distribution of a particular plane, the Schulz reflection method<sup>[4]</sup> with filtered CuK $\alpha$  radiation was used, and the results were displayed in pole figures.

## 2.4 Forming Limit Diagram

A visually detectable neck was used as the criterion for failure and the different strain combinations were obtained by varying the blank widths used in limiting dome height tests.

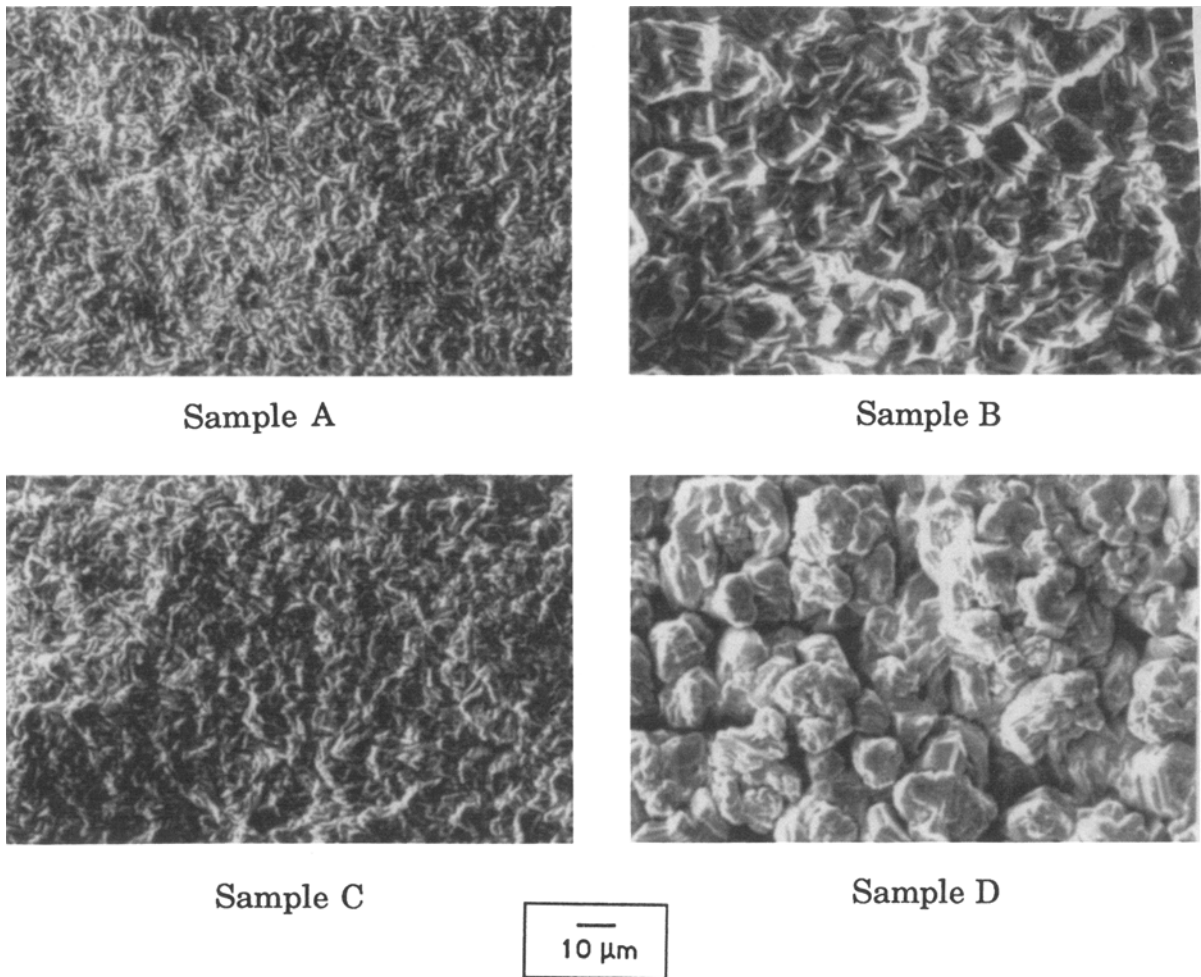


Fig. 2 Scanning electron micrographs of the surface of as zinc-coated samples at 500 $\times$ .

Table 3 Mechanical Properties of the Steel Substrate

Mechanical property	Location in coil							
	Head		Middle		Tail			
	<i>L</i>	<i>T</i>	<i>L</i>	<i>T</i>	<i>L</i>	<i>T</i>	<i>L</i>	<i>T</i>
Yield strength(a), MPa .....	170	175	174	183	190	189		
Tensile strength, MPa .....	308	306	311	305	310	306		
Total elongation, % .....	41.5	41.0	43.0	41.7	39.5	41.5		
<i>n</i> value .....	0.22	0.21	0.23	0.22	0.21	0.21		
Hardness, $R_{30T}$ .....		44.2		43.4		44.0		
Plastic, $r_m$ .....		1.63		1.60		1.59		
Anisotropy, $\Delta r$ .....		0.43		0.42		0.42		

Note: Tests on coated samples indicated that the coating did not affect the mechanical properties in uniaxial tensile test. (a) 0.2% offset yield.

### 2.5 Limiting Dome Height Tests

The limiting dome height tests were done using an MTS sheet-metal-forming system. All samples were 7 in. in the transverse direction. The punch used was a 4-in.-diameter ball bearing. The test procedures were generally in accordance with the North American Deep Drawing Research Group (NADDRG) Recommended Referee Practice established No-

ember 9, 1987. The tooling was cleaned with Scotch Brite and low-viscosity mineral seal oil before testing each set of samples and with the mineral seal oil between individual tests. The samples were cleaned with mineral spirits followed by low-viscosity mineral seal oil and run dry with the coated side in contact with the punch. The tooling was conditioned by running ten dummy blanks of the same type of material that was to be

tested. A punch speed of 10 in./min was used. Five samples were tested for each specimen width.

### 3 Results and Discussion

#### 3.1 Mechanical Properties

The mechanical properties are given in Table 3 and show little variance from head to middle to tail of the coil. These results indicated good processing practice for DQAK steel sheet. Tests on zinc-coated specimens showed that the coating had no effect on the mechanical properties. Therefore, in the following simulative forming tests, the steel substrate was invariant, and the effect of the surface could be isolated.

#### 3.2 Surface Morphology and Texture

The surface roughness ( $R_a$ ) and peaks per inch ( $P_c$ ) are listed in Table 4. The results presented were taken in the longitudinal and transverse directions. The uncoated steel and Sample A were similar in topography, as well as the smoother. Samples B, C, and D showed increasing roughness, respectively.

Figure 3 shows X-ray diffraction results of the four zinc coatings used in this study. The strongest eight reflections were

plotted and are represented in the figure. Samples A and C have strong prismatic orientations (basal plane normal to coating plane) and Samples B and D have high angle pyramidal orientations (basal plane  $61.7^\circ$  to coating plane). Figure 4 shows the percentage of grains with a particular orientation. The solid line drawn at 12.5% represents a random distribution of orientations. Samples A and C show the largest percentage of grains to have (10 $\bar{1}$ 0) and (11 $\bar{2}$ 0) planes oriented parallel to the coating plane (basal plane normal to coating plane). Samples B and D have the majority of grains with (11 $\bar{2}$ 2) planes lying parallel to the coating ( $61.7^\circ$  from basal plane), but Sample B has a higher percentage at 54%.

Figure 5 shows basal plane pole figures of the four zinc coatings. Samples A and C exhibit low basal intensities slightly increasing up to  $70^\circ$  to the coating plane, which is the angular limit of the Schulz reflection method. Samples B and D exhibit the highest intensities between  $40$  and  $60^\circ$ , which indicate the basal plane inclination angle relative to the coating plane. To provide a comprehensive representation of the (0002) pole figure data, the basal plane intensities measured in the radial direction were plotted as a function of basal plane inclination angle relative to the coating plane. Figure 6 is the plot for Samples A and C. Because  $70^\circ$  is the limiting angle, the dotted lines were

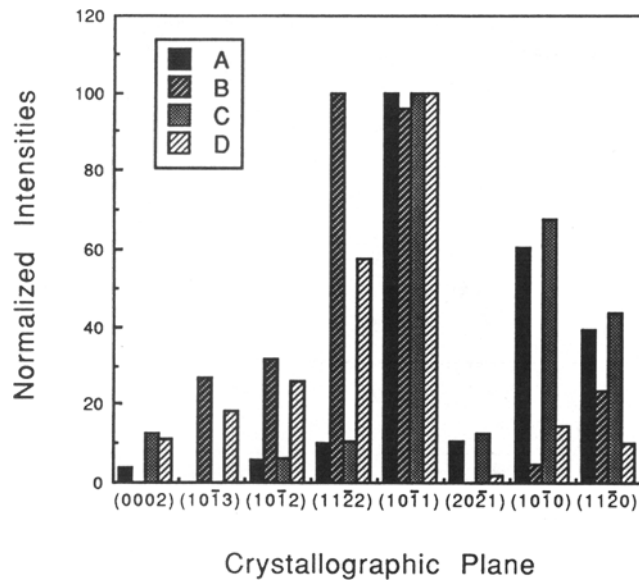


Fig. 3 Normalized Zn peak intensities.

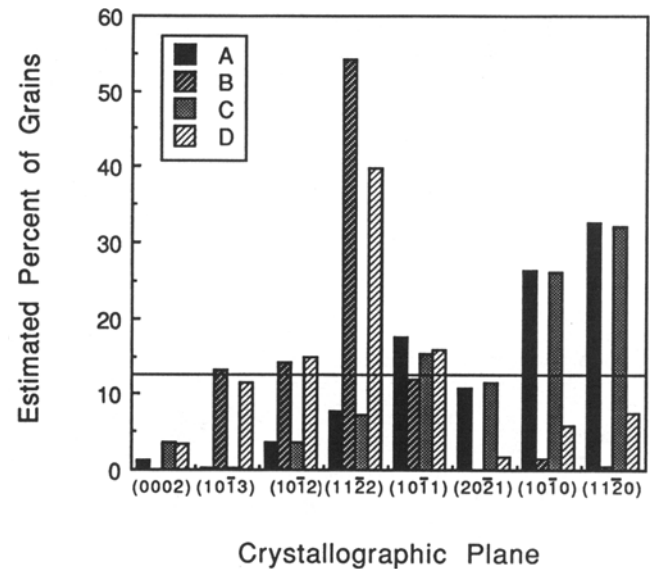


Fig. 4 Estimated percent of grains oriented with a particular crystallographic plane.

Table 4 Surface Topography of the Uncoated and the Zinc-Coated Samples

Sample	Surface roughness ( $R_a$ ), $\mu\text{m}$		Surface density ( $P_c$ ), peaks/mm	
	L	T	L	T
Uncoated .....	0.89	0.86	7	7
A .....	0.99	1.04	9	11
B .....	1.55	1.52	13	14
C .....	1.19	1.24	9	12
D .....	2.46	2.46	14	15

Note: Average of ten measurements.

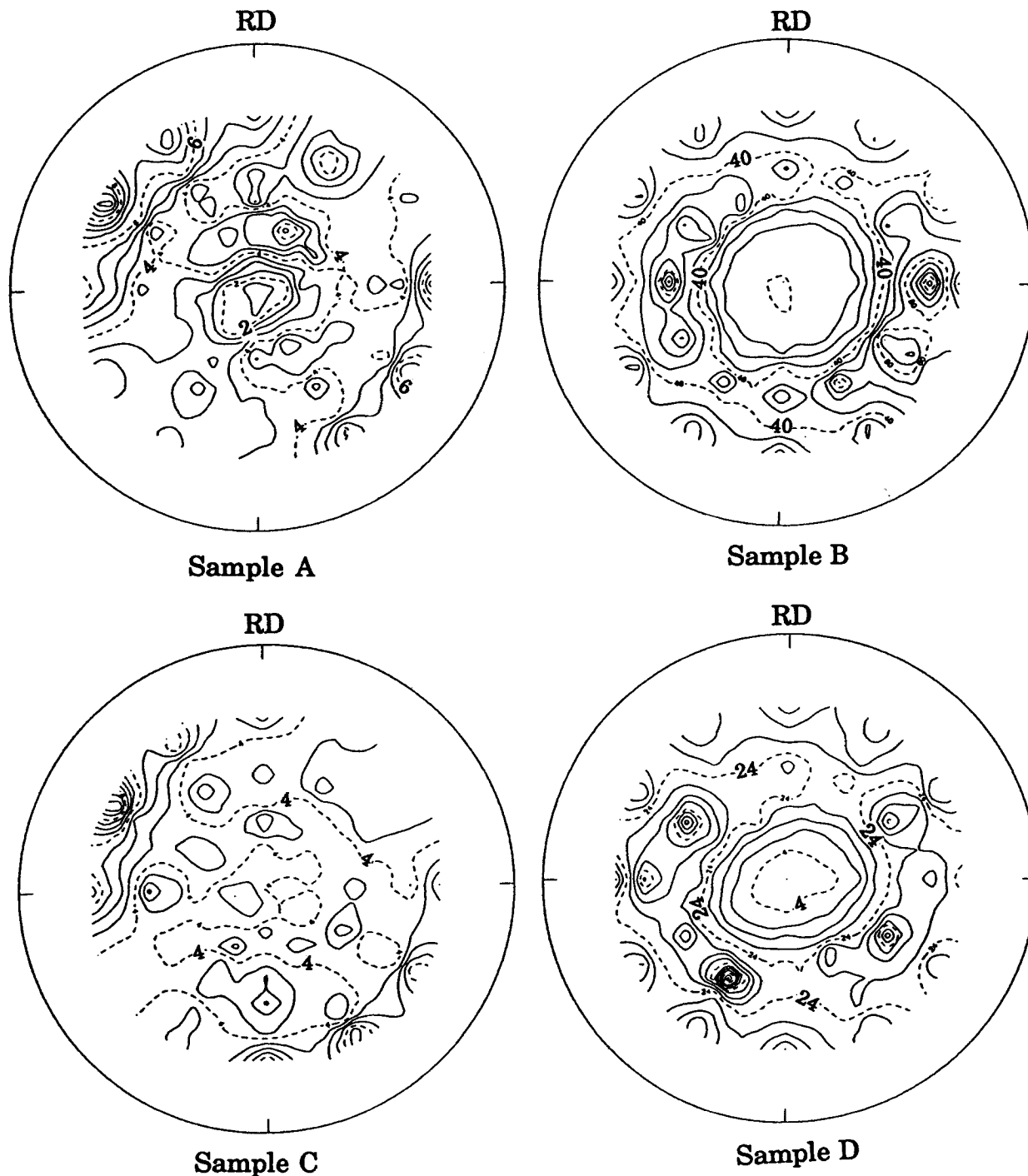


Fig. 5 Basal plane (0002) pole figure of electrodeposited zinc coatings.

drawn to show how the intensities may continue to rise to a maximum of  $90^\circ$ , which represents prismatic-type texture. The steeper slope of Sample A as it approaches  $90^\circ$  suggests that this sample will have a higher maximum intensity than Sample C, which means a more predominant prismatic-type texture. Figure 7 depicts basal plane intensity as a function of basal plane angle for Samples B and D. The figure shows that the maximum intensities are found between  $40$  and  $60^\circ$ , with Sam-

ple B having higher intensities and therefore indicating a stronger preferred pyramidal-type texture than Sample D.

### 3.3 Forming Limit Diagram

Figure 8 is a plot of the critical surface strains, which represents the onset of incipient localized necking for the uncoated sheet and the coated sheet. Because all of the points fall within

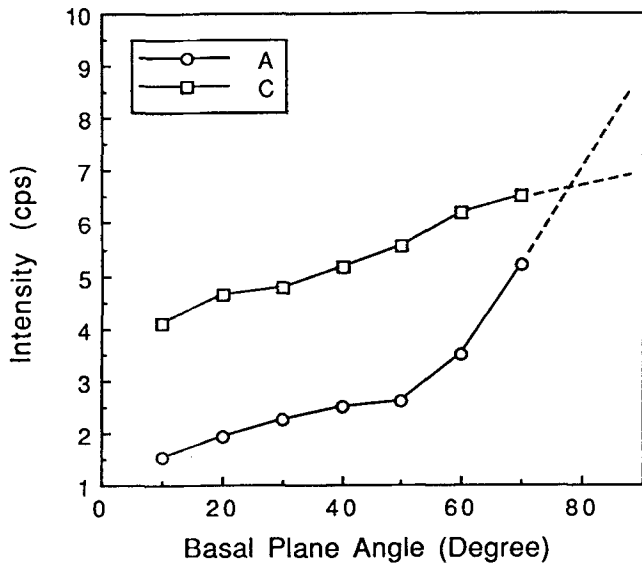


Fig. 6 Intensity as a function of basal plane angle for Zn-coated Samples A and C.

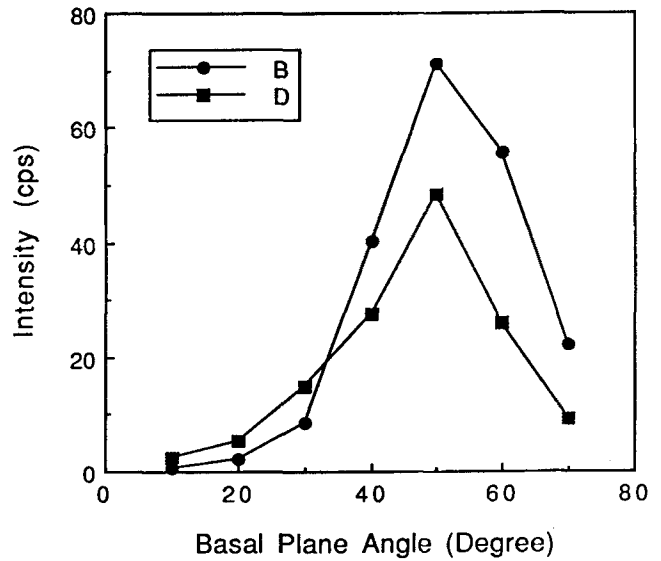


Fig. 7 Intensity as a function of basal plane angle for Zn-coated Samples B and D.

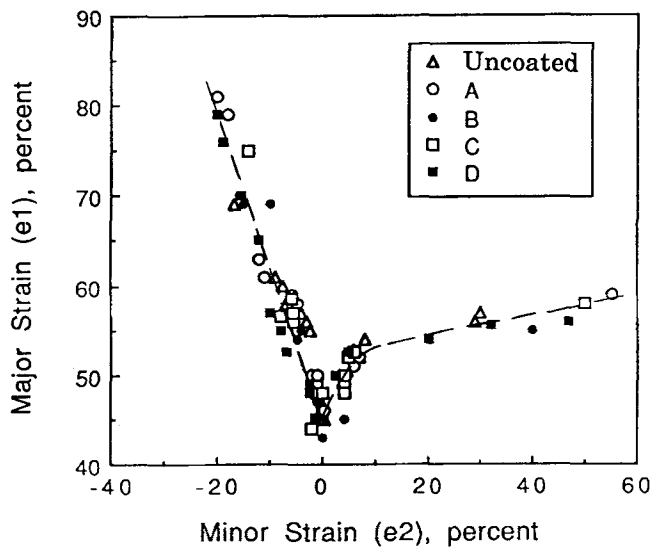


Fig. 8 Forming limit diagram of uncoated and Zn-coated DQAK sheet (0.74-mm thick).

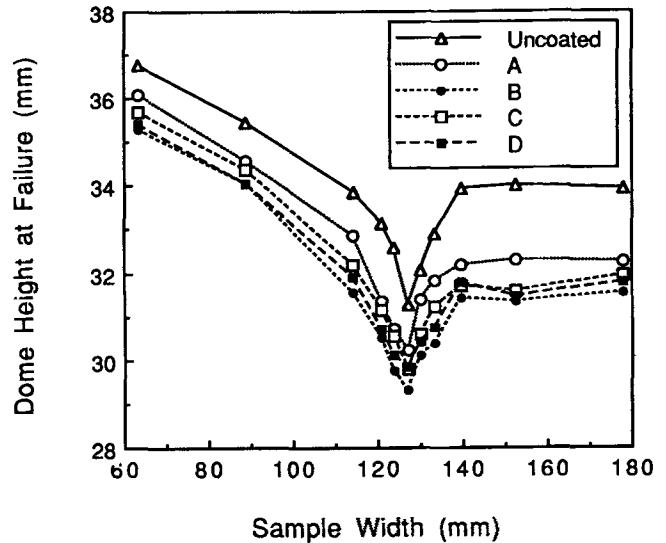


Fig. 9 Dome height at failure as a function of sample width.

the drawn curve, it can be concluded that these electrodeposited zinc coatings did not influence the forming limit diagram. However, although the limit strains were insensitive to the varying characteristics of the zinc coatings, the strain distribution did change, as evidenced by the different dome heights at failure obtained in limiting dome height tests.

### 3.4 Limiting Dome Height Tests

The limiting dome height results are shown in Fig. 9. Standard deviations for each set of five specimens at each specimen width ranged from 0.07 to 0.3 mm. For all tests, the uncoated sheet had the highest dome heights at failure. An explanation for this is that the coefficient of friction ( $\mu$ ) is the lowest for the case of the hard and smooth uncoated steel surface being in

contact with the hard ball bearing punch. The normal load contacting the asperities may be treated as an indentation in a hardness test, where the hardness is the normal load divided by the projected area of indentation. Because hardness is independent of the sum of the area of contact with the asperities, the real area of contact varies directly with normal load, and therefore,  $\mu$  is inversely proportional to hardness. Low interface friction results in a uniform distribution of strain, which yields higher limiting dome height values. The different hardness values of the coatings reported are a direct result of the different preferred orientations of the zinc grains. Because zinc is a close-packed hexagonal (cph) crystal, it is highly anisotropic, and preferred orientation is expected to influence limiting dome height values.

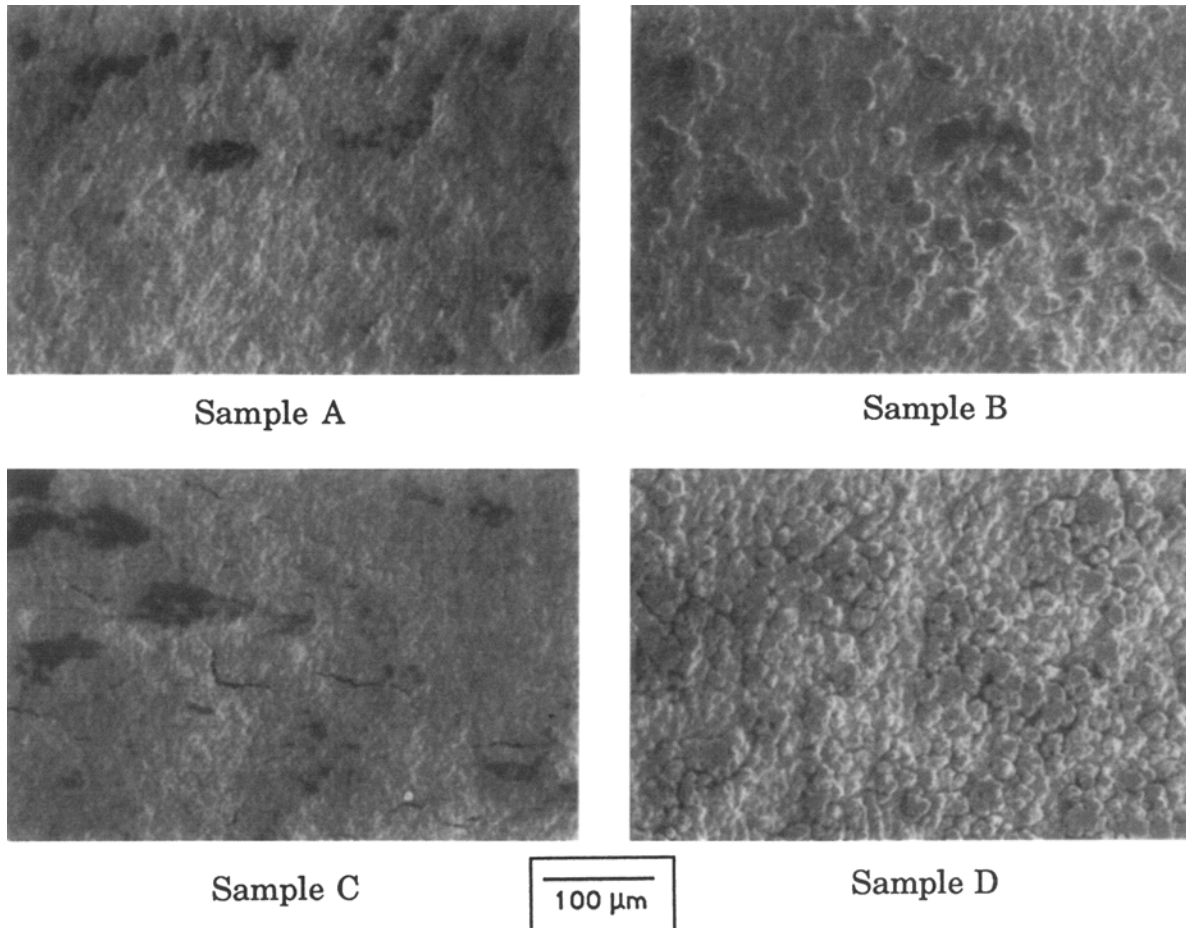
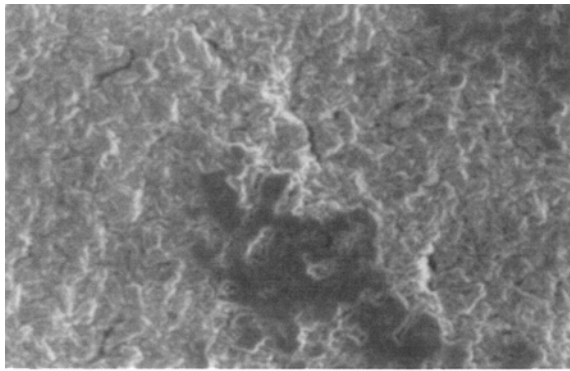


Fig. 10 Scanning electron micrographs taken at the pole of near plane-strain condition specimens showing punch contact area (150 $\times$ ).

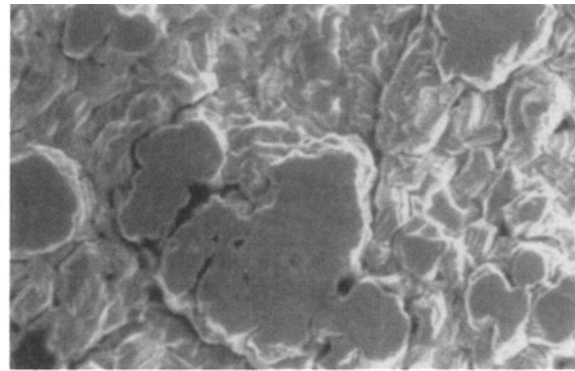
In an effort to explain the results of the zinc-coated samples, SEM photographs were taken at the pole of the contact region of the near plane-strain specimens and are shown in Fig. 10 and 11, at 150 $\times$  and 500 $\times$  magnification, respectively. Qualitatively, the photographs do not show a significant difference between deformed (contact) and undeformed regions for Samples A and C or for Samples B and D, but they indicate that the latter two have more contact region. Sample B had the lowest dome heights for all strain states, followed by Sample D. The fact that a greater fraction of surface was in punch contact may mean that a greater fraction of surface actually stuck to the punch, which required greater shear stress per unit normal pressure to cause slippage. Sample B was the softest coating as measured by the Knoop Hardness test and, therefore, more prone to plastic deformation from punch contact. Some zinc pickup was observed on the punch when running Sample B, which supports sticking friction and therefore the low limiting dome height values.

Figures 12 through 15 were plotted to isolate comparisons between coating thicknesses or weights and crystallographic textures and their effects on limiting dome height values. It was recently reported that zinc crystallographic texture influences

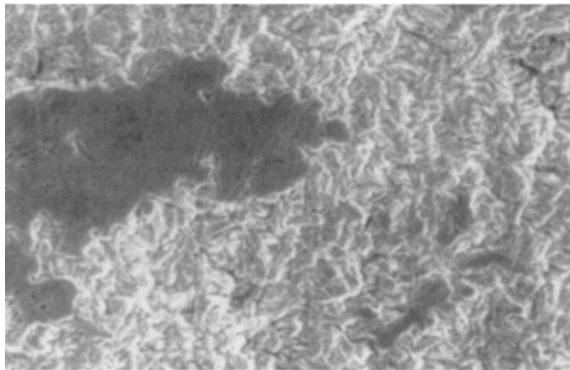
the coefficient of friction as measured using the draw-bead simulator test<sup>5,6</sup> The reported trend is that friction decreases in the textural sequence from basal to pyramidal to prismatic. The source of this behavior lies in the significant plastic deformation of the zinc coating during forming. Basal textured zinc has a higher resistance to deformation, which requires more plastic work per unit volume deformed. The results of this study also suggest that prismatic texture yields the lowest interface friction. Of the coated samples, Samples A and C (prismatic texture preference) had the higher dome heights at failure for all strain conditions. Figures 12 and 13 show that, for the same coating weights, the zinc samples with prismatic texture have higher dome heights at failure and, therefore, probably lower interface friction than the pyramidal textured samples. Figures 14 and 15 compare the two coating weights of each of the two textures, prismatic and pyramidal, respectively. Figure 14 shows Sample A to have higher dome heights than Sample C. Both zinc coatings had similar hardness and roughness characteristics, and the micrographs did not reveal any difference in fraction of area deformed. It is speculated that Sample A has a stronger prismatic-type texture, as given by the higher intensity slope as the basal plane inclination approaches 90 $^\circ$  in Fig. 6. Sample D, which



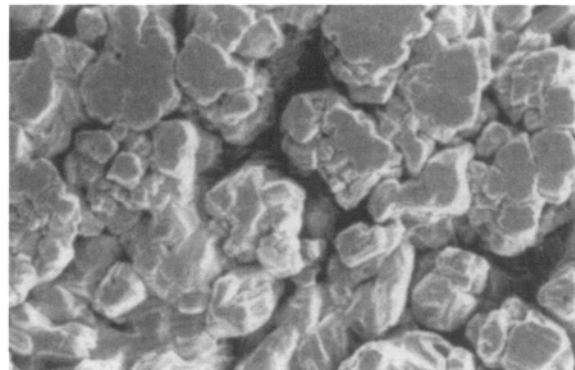
Sample A



Sample B



Sample C



Sample D

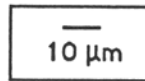


Fig. 11 Scanning electron micrographs taken at the pole of near plane-strain condition specimens showing punch contact area (500 $\times$ ).

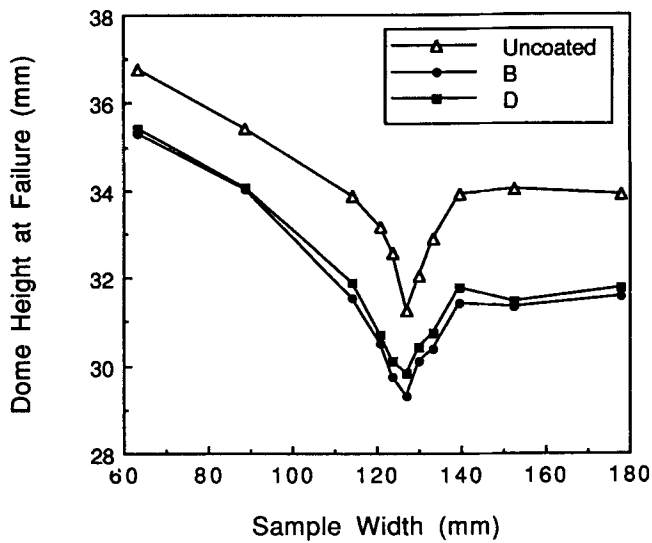


Fig. 12 Dome height at failure as a function of sample width for samples with 60-g/m<sup>2</sup> Zn coating weight.

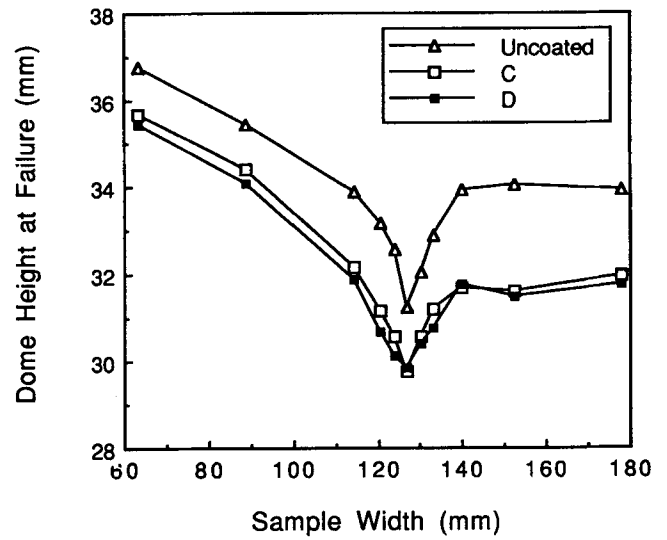


Fig. 13 Dome height at failure as a function of sample width for samples with 100-g/m<sup>2</sup> Zn coating weight.



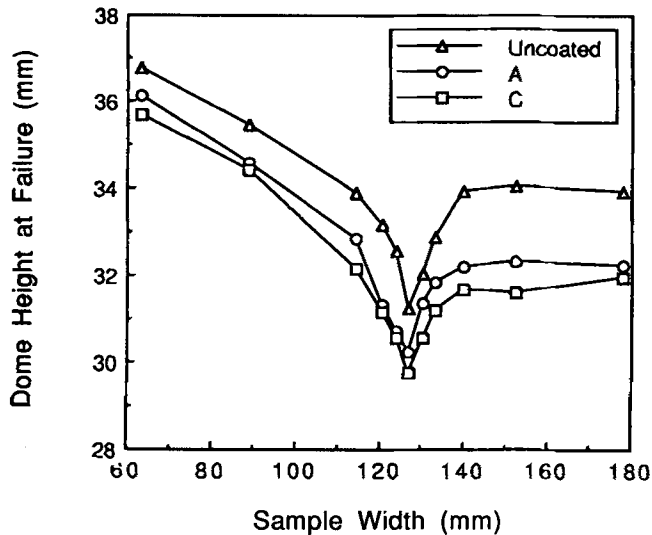


Fig. 14 Dome height at failure as a function of sample width for Zn-coated samples of prismatic texture.

had the roughest surface with an  $R_a$  value of  $2.46 \mu\text{m}$ , had greater dome heights at failure than its pyramidal textured partner, Sample B. Although its surface was rougher, it was also harder. In Fig. 4 and 7, Sample B was shown to have a stronger pyramidal texture preference than Sample D.

It should be noted that zinc coating thickness (weight) did not influence formability in this study. The lower coating weight sample had higher limiting dome height values for prismatic texture, and the reverse order held true for the pyramidal textured samples. It should also be noted, however, that the forming tests used in this work were on thoroughly cleaned specimens as recommended by the NADDRG. In production metal-forming, at least the mill-applied oil would be used, which could act as a lubricant and alter the friction at the tool/sheet interface.

## 4 Conclusions

Electrodeposited zinc coatings do not affect the forming limit diagram. Uncoated sheet steel has better formability as assessed by the limiting dome height than sheet with electrodeposited pure zinc coatings. The reason for this may stem from differences in tool/sheet interface friction. For the zinc coating weights investigated in this work, zinc coating weight does not influence formability. The preferred prismatic-type texture of zinc coating has been shown to enhance formability. This agrees with recent reports by Lindsay *et al.*<sup>[5]</sup> and Shaffer *et al.*,<sup>[6]</sup> which show prismatic textures to decrease the coefficient of friction. The zinc coating crystallographic texture may be as

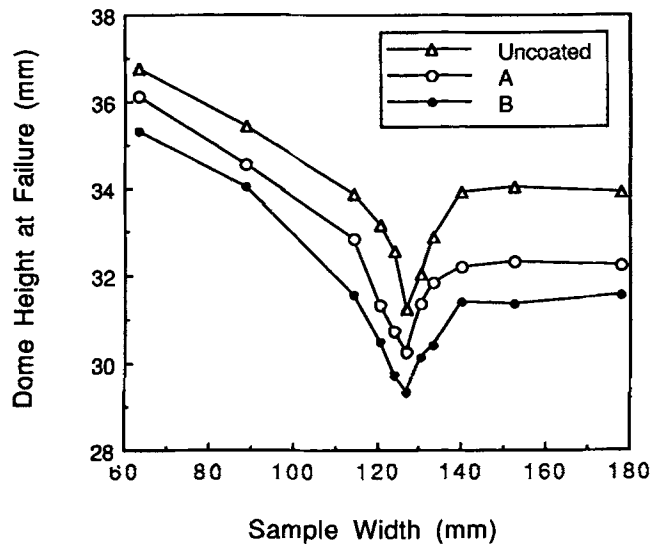


Fig. 15 Dome height at failure as a function of sample width for Zn-coated samples of pyramidal texture.

important as initial surface roughness in characterizing friction.

## Acknowledgments

The experimental assistance of J.E. Manack and L.E. Berta, Jr., of U.S. Steel in electroplating the panels; D.L. Crespy of U.S. Steel in running the LDH tests and S.W. Pak of Northwestern University in running the X-ray diffraction tests. A special thanks goes to H.M. Alworth, formerly of U.S. Steel, for his guidance and many helpful suggestions.

## References

1. H.M. Alworth and J.L. Milián, USS Research Internal Report, May 22 (1989).
2. A.K. Ghosh, *Met. Eng. Quart.*, 15, 53 (1975).
3. B.D. Cullity, *Elements of X-Ray Diffraction*, Addison-Wesley, Reading (1956).
4. L.G. Schulz, *J. Appl. Phys.*, 20, 1033-1036 (1949).
5. J.H. Lindsay, R.F. Paluch, H.D. Nine, V.R. Miller, and T.J. O'Keefe, *Plating Surf. Finish.*, Mar, 62-69 (1989).
6. S.J. Shaffer, W.E. Nojima, P.N. Skarpelos, and J.W. Morris, *Proc. TMS Symposium on Zinc-Based Steel Coatings Systems*, G. Krauss and D.K. Matlock, Ed., Detroit, Oct 7-11, 251-261 (1990).